ISSN 1062-7391, Journal of Mining Science, 2018, Vol. 54, No. 1, pp. 61–68. © Pleiades Publishing, Ltd., 2018.
Original Russian Text © B.F. Simonov, A.O. Kordubailo, V.Yu. Neiman, A.E. Polishchuk, 2018, published in Fiziko-Tekhnicheskie Problemy Razrabotki Poleznykh Iskopaemykh, 2018, No. 1, 71–78.

SCIENCE OF MINING MACHINES

Processes in Linear Pulse Electromagnetic Motors of Downhole Vibration Generators

B. F. Simonov[a]*, A. O. Kordubailo[a], V. Yu. Neiman[b], and A. E. Polishchuk[a]**

[a]*Chinakal Institute of Mining, Siberian Branch, Russian Academy of Sciences, Novosibirsk, 630091 Russia*
**e-mail: Simonov_BF@misd.ru*
[b]*Novosibirsk State Technical University, Novosibirsk, 630073 Russia*
***e-mail: nv.nstu@ngs.ru*

Received January 28, 2017

Abstract—The experimental research of processes running in a linear pulse electromagnetic motor of a downhole vibration generator is described. Based on the research findings, design requirements and recommendations on basic geometrical proportions of the equipment are formulated.

Keywords: Downhole vibration generator, percussive-action electromagnetic motor, blow energy and frequency, mechanical power.

DOI: 10.1134/S1062739118013353

One of the key targets of crude production is enhancement of oil recovery. Among numerous methods of reaching the objective, the most promising are vibration approaches. Vibration treatment is suitable both for bottom-hole area and a whole reservoir, and is combinable with all commonly known techniques of enhanced oil recovery. In this context, creation of equipment (vibration generators) to treat reservoirs and bottom-hole area yet remains of the current concern [1, 2].

Surface vibration sources tested in oil fields of Tyumen, Ural, Volga Region in the 1990s demonstrated high efficiency [3, 4]. Nonetheless, they found no wide application due to large size and complex operation of the equipment. At the present time, downhole vibration generators are being extensively developed [5, 6].

A promising approach appears to be creation of downhole vibration sources on the basis of electromagnetic motor for percussive machines as a linear pulse drive with a hydraulic power element. The latter converts axial movement of shaft being blown to radial movement of spacer assemblies that have effect on oil reservoir through well casing. The design and operation of the drive and power element are subject to some constraints connected with the well size. First, the drive should provide the required blow energy ($A_{\text{blow}} = 150 - 200$ J) at sufficiently small inside diameter R_2 ($2R_2 \le 110 - 115$ mm); second, hammering unit should have high back-off coefficient (to $K_0 = 0.85 - 0.95$). In order to reach such energy at limited radial size, it is necessary to lengthen power stroke of the hammer. Since the latter is connected with length of magnet coils, the newly created motors should agree with condition that $L_{\text{coil}} / R_1 > 12$, where L_{coil} is the length of coil; R_1 is the radius of cross section of hammering unit. The design features of such drives are described in [7, 8], which this article presents experimental research data on the dynamic processes running in electromagnetic motors and estimation of their impact on the motor design.

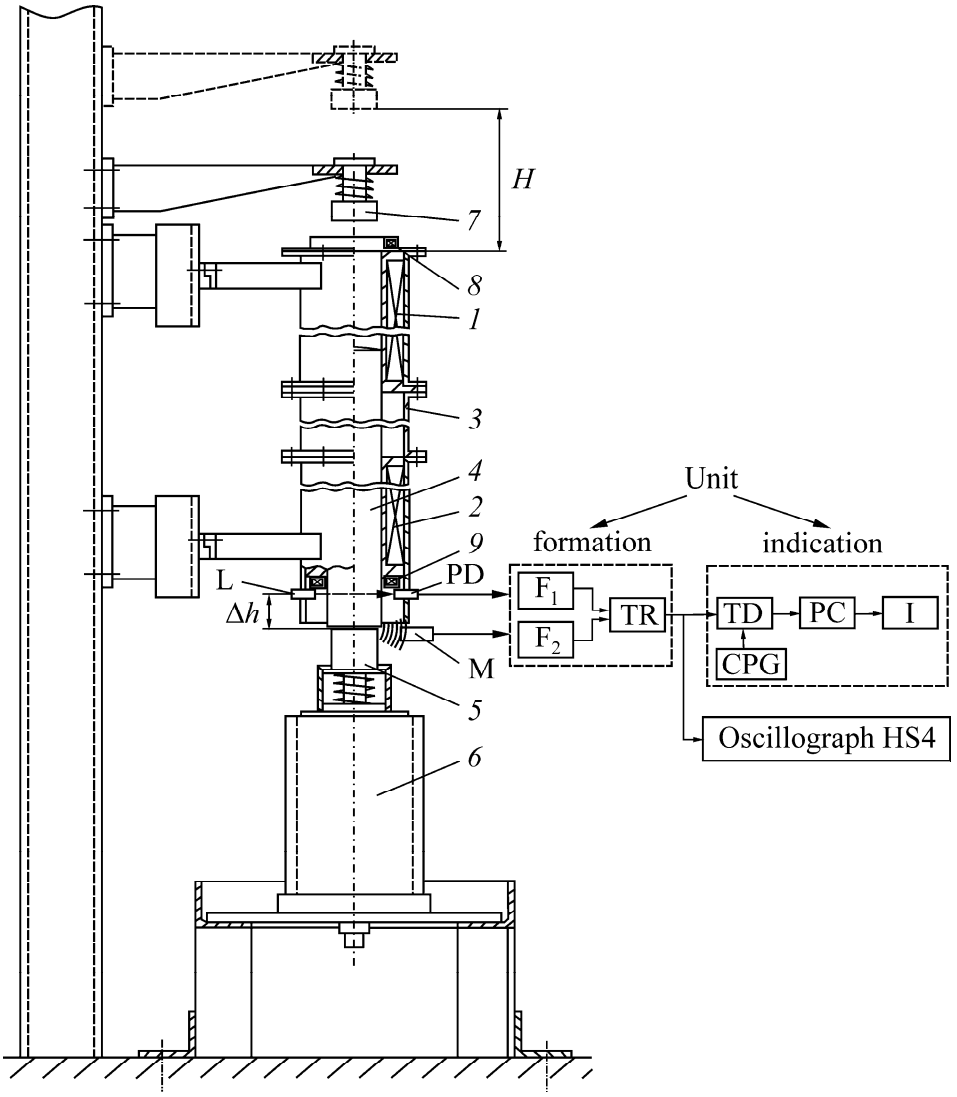

Fig. 1. Test bench with power element and electromagnetic percussion-type motor.

The studies were carried out on a test bench (Fig. 1) equipped with a power element and electromagnetic percussion-type motor. The motor is based on design of electromagnetic double-acting hammer and has two coils of idle run *1* and power stoke *2*; each coil has its own body with flanges connected by link *3*. Inside the coils, along a guide path, hammer *4* moves to and fro under the action of electromagnetic forces and delivers a blow on shaft *5* of power element *6* at the end of each cycle. In upward motion, the hammer decelerated by gravity and electromagnetic force of the power stroke coil. The height *H* (hammer travel length) is adjustable using stopper *7*. Switch of the coils is control by positions sensors *8*, *9* at the butts of the coils.

Coils are operated using the feed and control circuit (Fig. 2). The circuit represents a thyristor trigger with artificial commutation of electromagnetic coils L_1, L_2 using commutating capacitor C_3 dissipation of residual energy of switched-off coils on dissipation elements R_2C_2. Switch of the coils is executed by position sensors L_3, L_4. Actuation uses *Start* button SB_1 [9]. Voltage control is ensured by autotransformer T through the three-phase rectifying bridge $VD_1 - VD_6$.

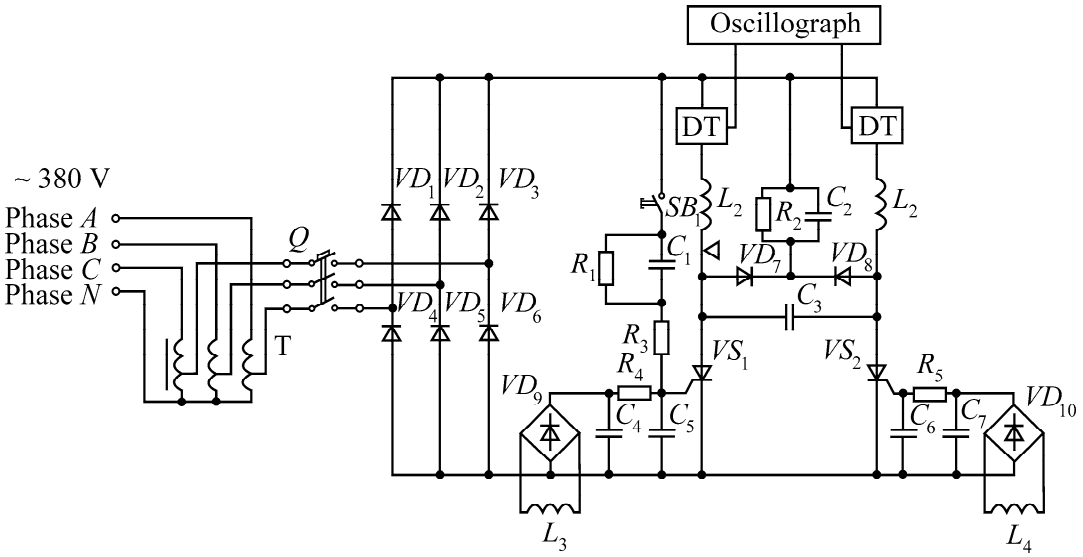

Fig. 2. Feed and control circuit of electromagnetic percussion-type motor.

The hammer velocity at the moment of blow was measured on the same bench (Fig. 1). In the head of the hammer, two opposite through holes are made for installation of laser L and photo diode PF. This pair makes a light sensor. In close vicinity to the blow point, microphone M is mounted. Signals from the light sensor and microphone go to a formation unit composed of pulse formers F_1, F_2 and trigger TR. An output of the former is recorded by oscillograph, while the output duration is displayed using an indication unit including time discriminator TD, countable pulse generator CPG, pulse counter PC and indicator I. This circuit enables tracking the time interval Δt from the moment when the hammer passes the light sensor to the moment of blow. Knowing the locating distance Δh, it is possible to calculate the hammer velocity at the blow moment: $V_{\text{blow}} = \Delta h / \Delta t$.

Dynamic characteristics were studied on two models of the same design electromagnetic motors (Fig. 1) with the parameters presented in Table 1 (R_1 is the hammer radius, $2R_2$ is the outer body diameter, m_{ham} is the hammer weight).

In such mode, long travel of the hammer in idle stroke is possible in case it is not limited by a stopper. For this reason, stopper *8* is included in the structure of the test bench (Fig. 1); it can be placed at an adjustable distance H from the upper pole of the idle stroke coil of the electromagnetic motor. In the tests, H was varied: $H = \infty$ (no stopper); $H = 138$ mm (stopper is in up position); $H = 20$ mm (stopper is in down position), in close vicinity to the pole.

Statistical pull characteristics of electromagnets of these motors, $F_{\text{em}}(i, \delta)$, calculated in FEMM [10, 11], and the experimental data are depicted in Fig. 3. Evidently, at the permissible pulse current density ($i \le 5$ A/mm^2), the current pulse amplitude is not higher than 40–50 A while the magnetic pull is 2–3 times higher than the mass of the test hammers: $F_{\text{em}} \ge G_{\text{ham}}$. These outcomes attribute certain features to the work cycle of the motors.

Table 1. Structural parameters of electromagnetic motor

Parameter	L_{coil}, mm	L_{ham}, mm	R_1, mm	$2R_2$, mm	L_{coil} / R_1	m_{ham}, kg
Variant 1	278	356	24	95	11.58	4.9, 7.8, 11.8, 13.6
Variant 2	605	1030	25	108	24.20	11.2, 13.5, 14.2, 20.0

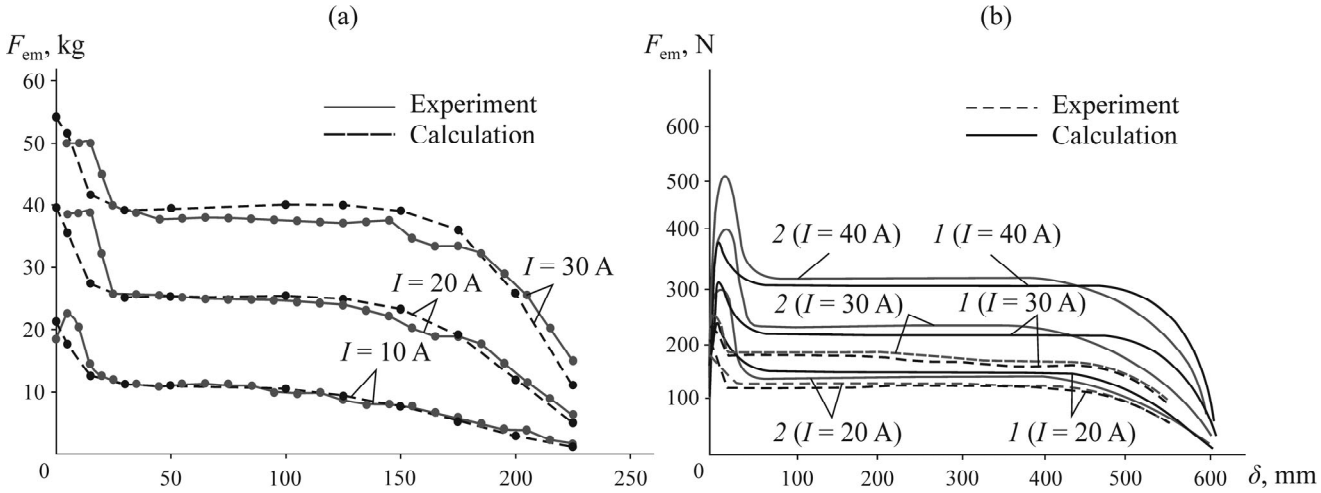

Fig. 3. Relationship of electromagnetic force $F(I, \delta)$, current i and magnet gaps δ for different variant motors: (a) variant 1 (L_{coil} = 268 mm, R_1 = 24 mm, W = 989 laps, S_{wire} = 2 mm^2); (b) variant 2 (*1*—hammer with small hole d = 10 mm, *2*—solid hammer, L_{coil} = 605 mm, R_1 = 25 mm, W = 1390 laps, S_{wire} = 4.4 mm^2); S_{wire}—wire area.

The tests of electromagnetic motor variant 1 estimated influence exerted on the work of the motor by the travel length of the constant weight travel controlled by the stopper and by the hammer weight m_{ham} without the stopper.

Figure 4 shows oscillograms of processes in the electromagnetic motor in case of variant 1, with $m_{ham} = 4.8$ kg without the stopper (Fig. 4a) and with the stopper in down position (Fig. 4b) at the distance $H = 20$ mm from the upper pole. From the comparison of the oscillograms it follows that when the stopper is absent $(H = \infty)$, in the idle stroke, the hammer travels beyond power stroke coil and current flows in the coil without the hammer and E.M.F. in it. In this case, the power stroke coil current i_2 stabilizes after reaching high values (Fig. 4a). At $H = 20$ mm, the head of the hammer never leaves the limits of the power stroke coil and the current i_2 (Fig. 4b), after jump at actuation, starts dropping up to the blow moment. Table 2 gives processing data for oscillograms of processes in this type motor.

The analysis of the data in Table 2 allows some conclusions to be drawn.

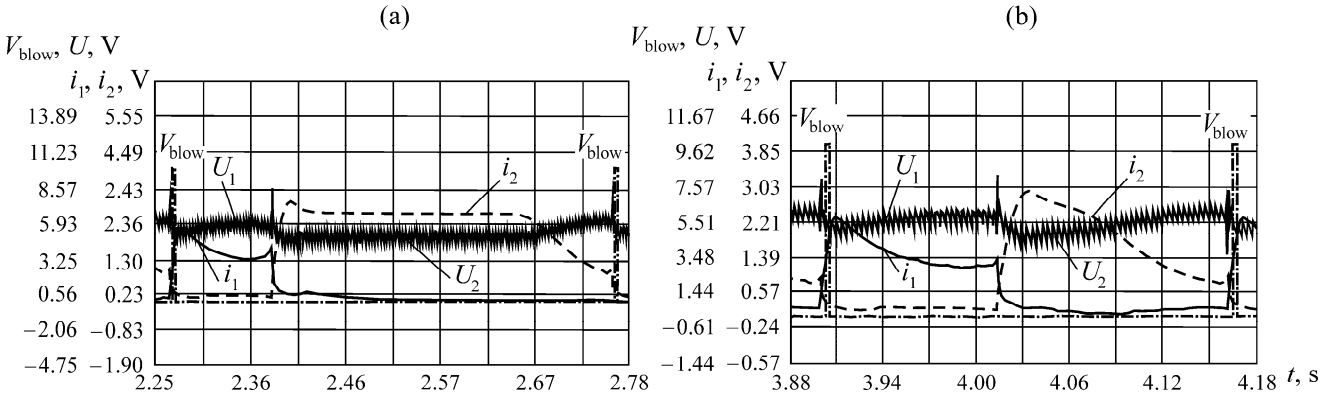

Fig. 4. Oscillograms of processes in variant 1 motor with the hammer 4.8 kg in weight, at the coil voltage of 65 V: (a) no stopper ($H = \infty$); (b) the stopper is in the down position at H = 20 mm (U_1, i_1; U_2, i_2 — respectively, voltages and currents of the idle and power stroke coils).

Table 2. Processing data for oscillograms of processes in motor of variant 1

H, mm	m_{ham}, kg	V_{blow}, m/s	i_{1max}	i_{2max}	W_1	W_2	W_Σ	A_{blow}	T_{blow}, s	f_{blow}, Hz	η, %	δ_{max}, mm	P_{mech}, W
			A			J							
∞	4.8	4.88	21.04	28.00	94.45	404.98	499.43	57.87	0.48	2.07	11.59	430	119.56
138	4.8	4.83	23.19	28.65	96.74	117.84	214.58	56.71	0.38	2.65	26.43	359	150.28
20	4.8	4.78	22.50	27.60	90.61	114.31	204.92	55.63	0.26	3.89	27.15	299	216.40

V_{blow} —blow velocity; i_{1max}, i_{2max} —amplitudes of currents in the idle and power stroke coils; W_1, W_2, W_Σ —energy consumed by the idle and power stroke coils, and total energy; A_{blow} —blow energy; T_{blow}, f_{blow} —period and frequency of blows; η —efficiency; δ_{max} —hammer travel amplitude; P_{mech} —mechanical power transferred to the power element: $P_{mech} = A_{blow} f_{blow}$.

The introduction of hammer stopper *8* and its arrangement closer to the upper pole of the upper coil (Fig. 1) when $F_{em} >> G_{ham}$ allows eliminating travel of the hammer head beyond the coil range and decreasing the hammer travel amplitude from 430 to 299 mm, as a result of which:

—the blow frequency is almost doubled (from 2.07 to 3.89 Hz);

—the blow energy A_{blow}, coil current amplitudes i_{1max}, i_{2max}, blow velocity V_{blow}, as well as the energies W_1 and W_2 consumed by the coils of idle and power strokes of the hammer, respectively, change insignificantly;

—the mains energy consumption is reduced by 60–70% as current flow in the power stroke coil is excluded when the hammer is not in it. The total efficiency η grows from 11.59 to 27.15%;

—the mechanical power of hammering P_{mech} grows from 119 to 216 kW (nearly 2 times) due to the higher blow frequency f_{blow} at $A_{blow} \approx \text{const}$.

Thus, in case that $F_{em} >> G_{ham}$ and $K_0 = 0.8 - 0.9$, it is expedient to add the design of the electromagnetic motor for the down-the-hole vibration generator with the stopper from above the hammer or to limit the vertical travel of the hammer so that it is inside the range of the power stroke coil, and, thereby, to enhance performance efficiency of the device.

The model of variant 1 is used to analyze operation of motors equipped with hammers of different weights $m_{ham} = \text{var}$ without a stopper $(H = \infty)$. The results compiled in Table 3 allow drawing conclusions that:

—until $F_{em} >> G_{ham}$, the amplitudes of the current pulses change insignificantly with the increasing hammer weight;

—while the hammer weight is increased at the same voltage of the coil, the condition $F_{em} >> G_{ham}$ is violated. The electromagnetic force approaches the hammer weight, and the hammer remains inside the range of the power stroke coil. In this case, the effect is the same as with the stopper, which results in the reduced energy consumption, higher efficiency, and increased mechanical power of hammering.

Table 3. Processed data of oscillograms of variant 1 motor operation with different weight hammers

H, mm	m_{ham}, kg	V_{blow}, m/s	i_{1max}	i_{2max}	W_1	W_2	W_Σ	A_{blow}	T_{blow}, s	f_{blow}, Hz	η, %	δ_{max}, mm	P_{mech}, W
			A		J								
∞	4.9	4.9	21.0	28.0	94.5	405.0	499.4	57.9	0.48	2.07	11.6	430	119.6
	7.8	4.6	22.0	27.8	111.7	393.6	511.3	81.0	0.54	2.00	15.8	420	162.4
	11.8	3.5	24.7	29.4	147.9	447.9	595.9	72.3	0.51	1.96	12.1	340	141.7
	13.6	3.2	31.0	33.2	124.0	225.0	350.0	69.0	0.31	3.14	19.7	310	216.6

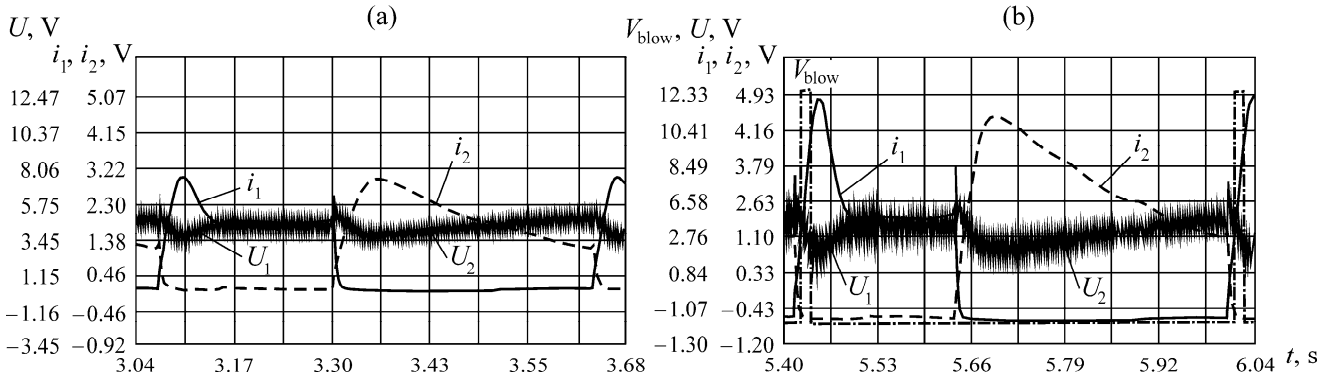

Fig. 5. Oscillogram of variant 2 motor operation: (a) hammer weight of 14.2 kg and $U = 65$ V; (b) hammer weight of 20.0 kg and $U = 80$ V.

In variant 2 motor, the coil voltage was not higher than limit: $U = U^*_{\text{lim}} = 100 - 110$ V, within which the hammer traveled beyond the idle stroke coil *1* (Fig. 1) not more than by 250 mm. At this travel length H, the entrance of the hammer in the power stroke coil range is zero, which is maximum permissible. Further increase in the voltage results in the hammer travel off the range of the power stroke coil and, thus, lower efficiency. This analysis was carried out for hammer of different weight (see Table 1).

Figure 5 shows the operation oscillograms for variant 2 motor with the hammer weight $m_{\text{ham}} = 14.2$ kg at the coil voltage $U = 65$ V and with $m_{\text{ham}} = 20.0$ kg at $U = 80$ V. The oscillograms for the hammer operation in case of $m_{\text{ham}} = 11.2$ and 13.5 kg are omitted. The latter hammers were of the same length as the hammer with $m_{\text{ham}} = 14.2$ kg but they were lightened owing to through axial holes made with diameters of 23 and 10 mm, respectively. The studies were carried out at the coil voltage $U \le U^*_{\text{lim}}$.

The research results are depicted in Fig. 6 as the relationship of coil voltage for different hammers and blow velocity V_{blow} (Fig. 6a), blow energy A_{blow} (Fig. 6b), motor efficiency η (Fig. 6c) blow frequency f_{blow} (Fig. 6d) and mechanical power $P_{\text{mech}} = A_{\text{blow}} f_{\text{blow}}$ (Fig. 6e).

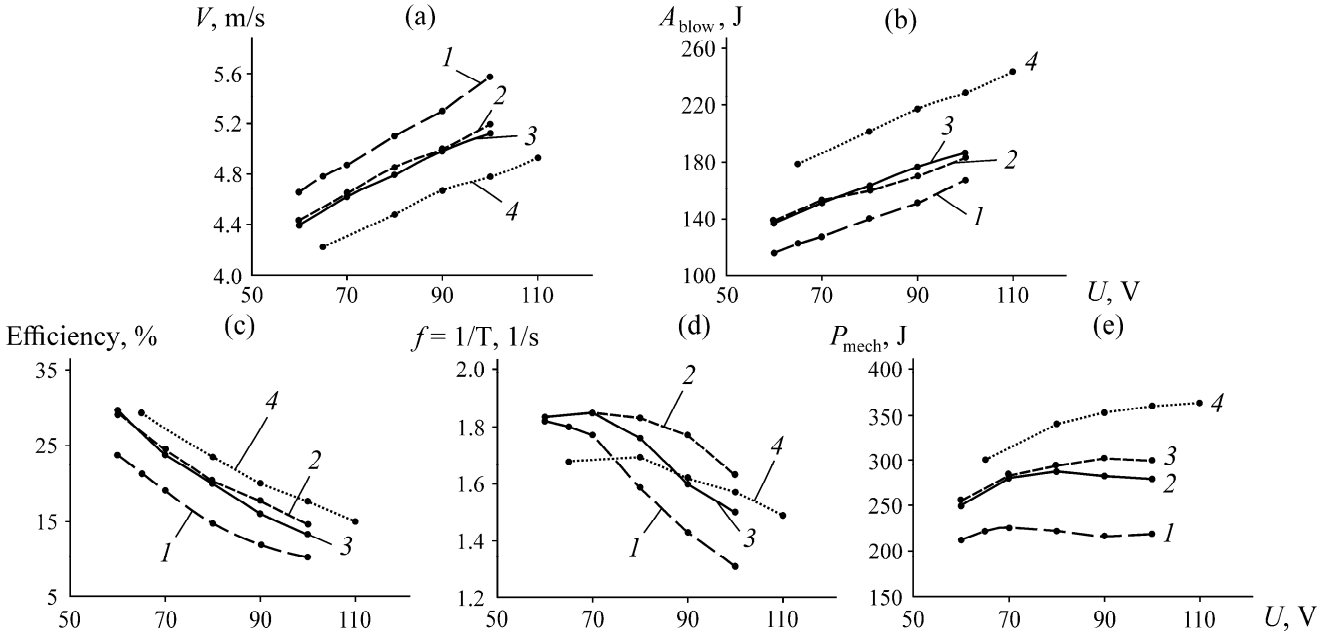

Fig. 6. Coil voltage for hammers with the weight $m_{\text{ham}} = 11.2$ (*1*), 13.5 (*2*), 14.2 (*3*), 20.0 kg (*4*) versus (a) blow velocity V_{blow}; (b) blow energy A_{blow}; (c) motor efficiency; (d) blow frequency; (e) mechanical power P_{blow}.

It follows from the analysis of the results at the same voltage on the electromagnetic percussion-type motor coils that the higher blow velocity is a feature of the lightest hammer with $m_{\text{ham}} = 11.2$ kg with a large axial hole, while the heaviest hammer with $m_{\text{ham}} = 20.0$ kg has the least blow velocity. The hammer with the small hole and $m_{\text{ham}} = 13.5$ kg, as well as the solid hammer with $m_{\text{ham}} = 14.2$ kg have the close-value blow velocities at the same voltage on coils.

The blow frequencies also depend on the coil voltage. Let us discuss three voltage ranges: low $60 \le U < 70$ V, medium $70 < U < 90$ V and high $U > 90$ V. In the low voltage range, the lighter hammers have the higher blow velocity. As the voltage is raised, the hammer travel lengthens in the idle stroke, which ends with the decreased blow frequency. The higher frequencies of blow are ensured by the heavier hammers with $m_{\text{ham}} = 14.2$ and 20.0 kg. The hammer with $m_{\text{ham}} = 20.0$ kg has the higher blow energy to 240 J. The hammers with $m_{\text{ham}} = 14.2$ and 13.5 kg have the same energies of blow, in the range of 140–180 J, as their weight are almost the same.

The lowest blow energy characterizes the hammer with the large axial hole and $m_{\text{ham}} = 11.2$ kg; the blow energy in this case ranges as 120–160 J but the efficiency is very low, 15–25%. The highest efficiency to 30% is provided by the hammer with $m_{\text{ham}} = 20.0$ kg. The hammers with $m_{\text{ham}} = 11.2$ kg and and $m_{\text{ham}} = 20.0$ kg feature the lowest and highest mechanical power, respectively. The electromagnetic percussion-type motor with the solid hammer with $m_{\text{ham}} = 14.2$ kg and the hammer with a small axial hole have close-value mechanical powers. The blow frequency of the motors ranges as 1.5–2.2 Hz. The most advisable frequency is 1.5–1.7 Hz at the coil voltage of 80 V.

CONCLUSIONS

The research implemented on model of electromagnetic percussion-type motors meant for operating as drives in downhole pulse vibration generators allows drawing some conclusions and formulating design standards.

For the creation of EM percussion-type motors with the double-action two-coil hammers having the outside diameter not more than 115 mm and the blow energy of 200–300 J, it is recommended to use electromagnets with the relative length $L_{\text{coil}} / R_1 \ge 20$ in case of the satisfied condition $F_{\text{em}} >> G_{\text{ham}}$.

To ensure high efficiency and mechanical power of percussion, the operating cycle of electromagnetic motors should be such that the hammer travel after the idle stroke is never beyond the range of the power stroke coil. This objective can be reached through limitation of the hammer travel using a stopper or another device to control the upward motion of the hammer, or by means of heavier hammers and proper election of coil voltage such that the hammer travel is limited by the hammer weight.

The inclusion of a solid hammer ort a hammer with a small-diameter through axial hole in the structure of the electromagnetic percussion-type motor changes the motor performance insignificantly. To this end, to ensure air flow through the hammer, the chosen axial hole size should meet the condition $d_{\text{hole}} / d_{\text{ham}} \le 0.25$.

REFERENCES

1. Oparin, V.N., Simonov, B.F. et al., *Geomekhanicheskie i tekhnicheskie osnovy uvelicheniya nefteotdachi plastov v vibrovolnovykh tekhnologiyakh* (Geomechanical and Technical Enhancement of Oil Recovery in Vibration Technology), Novosibirsk: Nauka, 2010.
2. Oparin V. N., Simonov B. F. Nonlinear Deformation-Wave Processes in the Vibrational Oil Geotechnologies, *J. Min. Sci*., 2010, vol. 46, no. 2, pp. 95–112.

3. Simonov, B.F., Serdyukov, S.V., Cherednikov, E.N., et al., Pilot Project Results on Enhancement of Oil Recovery by Vibro-Seismic Method, *Neft. Khoz.*, 1996, no. 5, pp. 48–52.
4. Simonov, B.F., Cherednikov, E.N., et al., Technology of Volume Wave Action on Oil and Gas Reservoirs to Enhance Hydrocarbon Recovery, *Nefty. Khoz.*, 1998, no. 4, pp. 42–44.
5. Oparin, V.N., Simonov, B.F., Savchenko, A.V., et al., Pulse Hydropercussion Technology and Equipment for Enhanced Oil Recovery, *Oil and Gas Euraisa*, 2012, no. 6, pp. 40–45.
6. Dyblenko, V.P., Marchukov, E.Yu., Tufanov, I.A., et al., *Volnovye tekhnologii i ikh ispol'zovanie pri razrabotke mestorozhdenii nefti s trudnoizvlekaemymi zapasami* (Wave Technologies and Their Application to Hard Oil Recovery), Book 1: RAEN, 2012.
7. Simonov, B.F., Kadyshev, A.I., and Neiman, V.Yu., Statistic Parameters of Long-Stroke Electromagnets for Hammers, *Transport: Nauka, Tekhnika, Upravl.*, 2011, no. 12, pp. 30–32.
8. Simonov, B.F., Neiman, V.Yu., and Shabanov, A.S., Pulsed Linear Solenoid Actuator for Deep-Well Vibration Source, *J. Min. Sci.*, 2017, vol. 53, no. 1, pp. 117–125.
9. Ryashentsev, N.P., Malov, A.G., and Nosovets, A.V., *Elektromagnitnye moloty* (Electromagnetic Hammers), Novosibirsk: Nauka, 1979.
10. Meeker, D., *Finite Element Method Magnetics, User´s Manual*, Ver. 4.0; June 17, 2004.
11. Bul', O.B., *Metody rascheta magnitnykh sistem elektricheskikh apparatov: Magnitnye tsepi, polya I program FEMM: ucheb. posob.* (Methods to Calculate Magnetic Systems of Electric Apparatuses: Magnetic Circuits, Fields and FEMM Program: Educational Aid), Moscow: Akademiya, 2005.